Proceedings of the 14th International Symposium on Process Systems Engineering – PSE 2021+
June 19-23, 2022, Kyoto, Japan

Dynamic Operability Analysis for the Calculation of Transient Output Constraints of Linear Time-Invariant Systems

San Dinh[a], Fernando V. Lima[a*]

[a]*West Virginia University, Morgantown, West Virginia, 26506, U.S.A*
**Fernando.Lima@mail.wvu.edu*

Abstract

In this work, a dynamic operability mapping is developed to find an operable funnel for a linear time-invariant dynamic system. The existing operability mapping method to find this funnel is computationally expensive, which makes it unsuitable for online control applications. A novel two-step calculation procedure is proposed, which includes an offline computation of the nominal funnel by constructing a convex hull of the manipulated variable projections, followed by an online update that adjusts the funnel to an operable region based on the current state information. As a result, a dynamic funnel that contains all achievable outputs regardless of the process disturbances and measurement noises is obtained in the form of transient output constraints for model predictive control implementation.

Keywords: Dynamic Operability, Linear Control, Output Constraints

1. Introduction

Process operability is defined as the design and control ability to achieve desired performance from the given available inputs regardless of the realization of the disturbances (Gazzaneo et al., 2020). If the operability analysis is able to be carried out along with the operation of a process, not only the achievable portions of the desired outputs are known, but also the feasible output constraints can be provided for model predictive control to guarantee feasibility (Lima and Georgakis, 2009). However, the currently available operability analysis involves an exhaustive generation of the input combinations, and thus this approach may quickly become intractable.

In this paper, the achievable output sets at all values of the disturbances are formulated as a set of time-dependent polyhedra, which is referred to as the dynamic operable funnel. To avoid confusion between control theory and process operability concepts, external output constraints are defined here as the constraints on the output variables that are given by the physical nature of a process, such as thermodynamic and equipment's safety limits. In the application to online model predictive control, the dynamic funnel provides the transient output constraints to keep the process from moving toward an inoperable region, and the online calculation must be done efficiently to assure a sufficient time for the controller to solve for an optimal path.

In particular, the dynamic operable funnel of a linear time-invariant dynamic process is proven to be defined as a polyhedron. Also, the ability of the current process to move toward its stable operating region is quickly verified following Phase I of the simplex algorithm for linear programming, and the operable region in the presence of external output constraints can be obtained via the convex hull of suitable geometric duals with respect to a feasible solution (Muller and Preparata, 1978). Therefore, the remaining challenge is constructing the dynamic operable funnel in a tractable manner. In the proposed framework, the funnel calculation is divided into two steps: the first step is computing the funnel offline before the full state information arrives; and the second step is updating the funnel online according to the full state information that becomes available. The preliminaries and concepts necessary to define the proposed approach are detailed next.

2. Dynamic Operability Problem Background

2.1. Preliminaries

Consider the following discrete-time linear time-invariant dynamic system:

$$x(k+1) = Ax(k) + Bu(k) + Gw(k);\ x(0) = x_0 \tag{1}$$

$$y(k) = Cx(k) + Du(k) + v(k) \tag{2}$$

in which $x(k) \in \mathbb{R}^{n_x}, u(k) \in \mathbb{R}^{n_u}\ and\ y(k) \in \mathbb{R}^{n_y}$ are the vectors of state variables, input/manipulated variables and output/controlled variables, respectively; $w(k) \in \mathbb{R}^{n_w}$ and $v(k) \in \mathbb{R}^{n_v}$ are the zero-mean multivariate Gaussian distributed vectors with the respective positive definite covariance matrices, $\Sigma_w \in \mathbb{R}^{n_w \times n_w}$ and $\Sigma_v \in \mathbb{R}^{n_v \times n_v}$. The initial time $k = 0$ is defined to be the current time instead of the time in which the process begins, and the initial state variables, x_0, are assumed to be given by a state observer.

Since $w(k)$ and $v(k)$ are assumed to be zero-mean with Gaussian distributions, the states and the outputs are also multivariate Gaussian random variables with the respective means $\bar{x}(k)$ and $\bar{y}(k)$. The sequences of covariance matrices for the states, $\Sigma_x(k)$, and the outputs, $\Sigma_y(k)$, are:

$$\Sigma_x(k+1) = A\Sigma_x(k)A^T + G\Sigma_w G^T; \Sigma_x(0) = 0_{n_x \times n_x} \tag{3}$$

$$\Sigma_y(k) = C\Sigma_x(k)C^T + \Sigma_{\text{v}} \tag{4}$$

When a random vector $p \in \mathbb{R}^{n_p}$ is a Gaussian random vector with a mean $\bar{p}$ and a covariance matrix Σ_p, its 95% highest density region, $HDR(p)$, is the following ellipsoid with the scale l_p^2 equals to the inverse cumulative distribution function of the chi-squared distribution with n_p degrees of freedom:

$$HDR(p) = \left\{p|(p-\bar{p})^T \Sigma_p^{-1}(p-\bar{p}) \leq l_p^2; l_p^2 = Inv_{\chi^2}(95\%; n_p)\right\} \tag{5}$$

2.2. Dynamic operability sets

The Available Input Set at the discretized time k (AIS_k) is defined as the set of all feasible sequences of manipulated variables from the initial time 0 to time k.

$$AIS_k = \left\{u_k = [u(0)^T, u(1)^T, \dots, u(k-1)^T]^T | u_{k,min} \leq u_k \leq u_{k,max}\right\} \tag{6}$$

The Expected Disturbance Set (EDS_k^d) is the set of all realizations of the disturbances, d, at the time k. The two sources of disturbances assumed here are the $w(k)$ and $v(k)$, which can take any real values due to their Gaussian distributions. Their values are constrained to their respective 95% highest density regions as follows:

$$EDS_k^d = \left\{ d(k) = [w(k)\ v(k)]^T \middle| \begin{matrix} d(k)^T diag(\Sigma_w^{-1}, \Sigma_v^{-1}) d(k) \le l_d^2 \\ l_d^2 = Inv_{\chi^2}(95\%; n_w + n_v) \end{matrix} \right\} \tag{7}$$

The Achievable Output Set at a fixed disturbance d ($AOS(d)$) is the set of all possible outputs at the discretized time k given the linear system (1), (2) and the range of manipulated variables. A necessary condition for a process to be operable is that the set of achievable outputs regardless of the realizations of the process disturbances, AOS_k, has to be nonempty. The AOS_k is defined as the intersection of all achievable output sets at fixed realizations of the disturbance:

$$AOS_k = \bigcap_{d \in EDS_k^d} AOS_k^d(d) = \left\{ y(k) \middle| \begin{matrix} (1), (2)\ are\ satisfied; \\ u_k \in AIS_k; d(k) \in EDS_k^d; \end{matrix} \right\} \tag{8}$$

3. Calculation of Transient Output Constraints

3.1. Offline computation of transient state funnel at nominal-valued disturbances

The following assumptions are considered for the offline calculation of the dynamic funnel that can be later addressed in the online update: $x_0 = 0_{n_x}; C = I_{n_x \times n_x}; D = 0_{n_x \times n_u}$; $w(i) = 0_{n_w}; v(i) = 0_{n_x}\ \forall\ i \le k$. The considered outputs are the predicted state variables before $w(k)$ and $v(k)$ are accounted for, and the AOS_k has the form:

$$AOS_k = \{x(k) | x(k) = \bar{B}_k u_k; u_k \in AIS_k\} \tag{9}$$

where $\bar{B}_k = [A^{k-1}B\ A^{k-2}B \dots AB\ B]$. From the definition (6), the AIS_k is a bounded convex polyhedron. From the formulation of (9), $\bar{B}_k : \mathbb{R}^{k \times n_{nu}} \to \mathbb{R}^{n_x}$ is a linear transformation of the AIS_k into the AOS_k, so that the AOS_k is exactly the smallest convex hull that contains all the projections of the available input sequences on the state vector space. Additionally, for an achievable state $x(k)$ to be a vertex of the AOS_k, its preimage, u_k, must be a vertex of the AIS_k. Then the AOS_k can be computed by taking the convex hull of the $2^{k \times n_u}$ vertices of the AIS_k, which is the vector of the input sequence in which each element is either taken from the value of the lower bound $u_{k,min}$ or the upper bound $u_{k,max}$:

$$AOS_k = convexhull\left(\bar{B}u_k | u_k^T e_i \in \{u_{k,min}^T e_i, u_{k,max}^T e_i\}, \forall i \le k \times n_u\right) \tag{10}$$

where $e_i = [0,0,\dots,0,1,0,\dots,0]^T \in \mathbb{R}^{k \times n_u}$ is a standard basis for which only the i^{th} location has the value of 1. An efficient approach to find the convex hull in high-dimensional spaces is the Quickhull Algorithm (Barber et al., 1996). According to the Minkowski-Weyl's Theorem, every polyhedron is identically described by its vertex representation and its hyperplane representation, and thus the formulation of AOS_k in (10) can be equivalently converted to a set of linear constraints using the Double Description Method (Fukuda and Prodon, 1996):

$$AOS_k = \{x(k) | \bar{H}_k x(k) \le \bar{l}_k\} \tag{11}$$

In the simplest case of the online calculation, if the process disturbances and the measurement noises are not considered, the online update of the dynamic funnel can be established by the substitution of (11) into the state-space model (1), and the dynamic funnel at the current state x_0 is simply:

$$AOS_k = \{x(k)|\bar{H}_k x(k) \leq \bar{\bar{l}}_k; \bar{\bar{l}}_k = \bar{l}_k + \bar{H}_k A^k x_0\} \quad (12)$$

3.2. Transient state funnel with process disturbances

In this subsection, the interested outputs are the state variables, and the following assumptions are considered: $C = I_{n_x \times n_x}; D = 0_{n_x \times n_u};\ v(i) = 0_{n_x}, \forall\ i \leq k$. The process disturbance sequence can be redefined as the deviation, $w_x(k)$, from the mean value of the state vector, and the EDS is chosen as the HDR with respect to $x(k)$:

$$EDS_k^x = \{w_x(k)|w_x(k)^T \Sigma_x^{-1}(k) w_x(k) \leq l_x^2; l_x^2 = Inv_{\chi^2}(95\%; n_x)\} \quad (13)$$

The formulation of AOS_k in this subsection is

$$AOS_k = \bigcap_{w_x(k)\,\in\, EDS_k^x} AOS_k^w(w_x(k)) = \left\{x(k) \middle| \begin{array}{c} x(k) = A^k x_0 + \bar{B}_k u_k + w_x(k) \\ u_k \in AIS_k; w_x(k) \in EDS_k^x; \end{array} \right\} \quad (14)$$

Let $\Sigma_x(k) = V_x(k) S_x(k) V_x^{-1}(k)$ be the eigenvalue decomposition of the covariance matrix $\Sigma_x(k)$. Since a basic property of any covariance matrix is positive definiteness, $V_x^{-1}(k) = V_x^T(k)$ is an orthogonal matrix, and $S_x(k)$ is a diagonal matrix with positive elements. Denoting $S_x^{-0.5}(k)$ to be an inverse of the square root of $S_x(k)$, a bijective mapping $L = S_x^{-0.5}(k) V_x^T$ that transforms the state vector $\hat{x}(k) = Lx(k)$ is introduced. The covariance matrix of the transformed vector $\hat{x}(k)$ is:

$$\Sigma_{\hat{x}}(k) = L\Sigma_x(k)L^T = S_x^{-0.5}(k) V_x^T V_x(k) S_x(k) V_x^T(k) V_x(k) S_x^{-0.5}(k) = I_{n_x \times n_x} \quad (15)$$

Because the covariance $\Sigma_{\hat{x}}$ is an identity matrix, the proposed linear mapping L corresponds to a change of coordinates to transform the state vector into a standard Gaussian random vector, and the ellipsoid EDS_k^x is transformed into an n-sphere $EDS_k^{\hat{x}}$ with radius l_x. This provides an advantage when finding the intersection AOS_k of all achievable output sets for the disturbance realizations based on the following theorem:

Theorem 1: Let $[H]_i$ denote the i^{th} row of a matrix $H: \mathbb{R}^{n_1} \to \mathbb{R}^{n_2}$. Given a bounded polyhedron in the form of $P_x = \{x \in \mathbb{R}^{n_x}|Hx \leq l\}$ and its image under a bounded translation according to an n-sphere $P_x(d) = \{\hat{x}|\hat{x} = x + d; Hx \leq l; d^T d \leq l_d^2\}$, the intersection of all $P_x(d)$ is given by:

$$P = \bigcap_{d^T d \leq l_d^2} P_x(d) = \left\{x \middle| Hx \leq \hat{l}; [\hat{l}]_i = [l]_i - l_d\sqrt{[H]_i^T [H]_i}\ \forall\ i \leq n_2 \right\} \quad (16)$$

Proof: For each hyperplane $[H]_i x \leq [l]_i$, the hyperplane $[H]_i x \leq [l]_i - l_d\sqrt{[H]_i^T [H]_i}$ is the parallel hyperplane shifted toward the feasible half-space by a distance of l_d. Thus, a translation of all feasible points in $[H]_i x \leq [l]_i$ by a distance d can only violate $[H]_i x \leq [\hat{l}]_i$ if $d > l_d$. Therefore, $Hx \leq \hat{l}$ is the intersection of all hyperplanes $[H]_i x \leq [l]_i$ when the translation distance is less than or equal to l_d.

Note that the disturbance effects on the state vector are the same as translating the achievable output set in (12) by a translation vector in EDS_k^x, and the linear mapping L puts the AOS_k^w in the form that is applicable for Theorem 1. Finally, since L is a bijective mapping, the final form of the transient state funnel with process disturbances in the original state vector $x(k)$ is given by:

$$AOS_k = \left\{x(k) \middle| \bar{H}_k x(k) \le \hat{l}_k; [\hat{l}_k]_i = [\bar{l}_k + \bar{H}_k A^k x_0]_i - l_x \sqrt{[\bar{H}_k L^{-1}]_i^T [\bar{H}_k L^{-1}]_i} \right\} \quad (17)$$

3.3. Transient output funnel with process disturbances and measurement noises

The output vector can be interpreted as a projection of the state variables and the manipulated variables at the same time step. Similarly to the previous subsection, using the Double Description Method, all the vertices of AOS_k in the state vector space can be found. Following the same procedure from (10) to (12), one can arrive at the achievable output set with process disturbances before considering the measurement noises:

$$AOS_k(v(k) = 0) = \{y(k) | H_k y \le \bar{b}_k\} \quad (18)$$

Since the effects of the measurement noises on the outputs are the same as the disturbances on the state variables, a similar procedure from (13) to (17) can be followed with the linear mapping $L_y = S_y^{-0.5}(k) V_y^T(k)$ defined according to the eigenvalue decomposition of $\Sigma_y(k) = V_y(k) S_y(k) V_y^{-1}(k)$. The final form of the achievable output set is:

$$AOS_k = \left\{y(k) \middle| H_k y \le b_k; [b_k]_i = [\bar{b}_k]_i - l_y \sqrt{[H_k L_y^{-1}]_i^T [H_k L_y^{-1}]_i} \right\} \quad (19)$$

4. Numerical Example

Consider the system given in (1), (2) with the following matrices:

$$A = \begin{bmatrix} 0.59 & -0.43 \\ -0.06 & 0.39 \end{bmatrix}; B = \begin{bmatrix} 0.42 & 1.82 \\ 2.48 & -0.71 \end{bmatrix}; G = \begin{bmatrix} 0.52 & -0.47 \\ 1.22 & 0.47 \end{bmatrix};$$
$$C = \begin{bmatrix} 0 & 1 \\ 1 & 1 \end{bmatrix}; D = 0_{2\times2}; \Sigma_w = \begin{bmatrix} 0.04 & 0 \\ 0 & 0.02 \end{bmatrix}; \Sigma_v = 10^{-5} \begin{bmatrix} 5 & 0 \\ 0 & 1 \end{bmatrix}; x_0 = \begin{bmatrix} 20 \\ -30 \end{bmatrix} \quad (20)$$

The prediction horizon is chosen to be 6 for illustrative purposes, and the objective is constructing the six achievable output sets AOS_k for $k = 1, \dots, 6$. The input ranges of the considered AIS_k are $-1 \le u_1(k) \le 1$ and $-2 \le u_2(k) \le 2$. In the offline computation, the vertices of the AIS_k, which are all combinations of $u(k) \in \{[-1\ -2]^T, [-1\ 2]^T, [1\ -2]^T, [1\ 2]^T\}$ for all $0 \le k \le 5$, are applied to the linear state-space model to calculate the associated basis state vectors. The set of convex hulls of these basis state vectors at each time k is the nominal AOS_k, and the funnel of nominal state vectors obtained for this case is shown in Figure 1(a).

In the online update of the dynamic funnel, at each value of k, the AOS_k is adjusted according to (12), and the new dynamic funnel at $w(k) = 0$ and $v(k) = 0$ is shown in Figure 1(b). To find the intersection of all AOS_k at different values of $w(k)$ in the 95% highest density region, (17) is applied, and the new AOS_k that takes into account process disturbances, $w(k)$, is shown as the dashed-edge empty polytopes in Figures 1(c) and (d). In the next step, AOS_k of state vectors are projected into the space of the output vectors, and the convex hulls of the images at every time k is the AOS_k of output vectors, which is represented as the dashed-edge empty polytopes in Figures 1(e) and (f). Finally, to address the measurement noise, the hyperplanes of every AOS_k are shifted inward according to (19). The result is a funnel of output vectors that can always be achieved regardless of the realization of the process disturbances and the measurement noises by varying the constrained manipulated variables. This funnel is plotted with dotted-edge grey-filled polytopes in Figures 1(e) and (f).

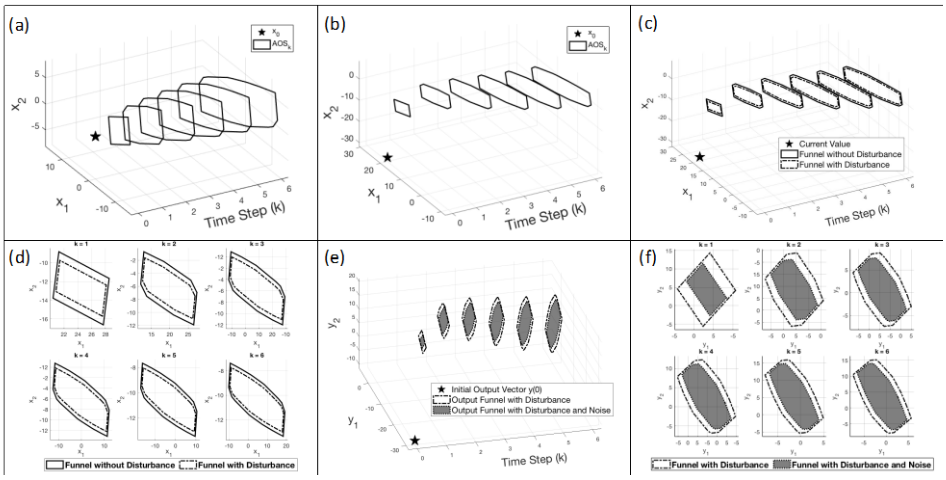

Figure 1: Dynamic operable funnels. (a): Funnel of state vector considering nominal initial state; (b): Funnel of state vector considering actual initial state without disturbances; (c), (d): Adjustment of funnel of state vectors with process disturbances; (e), (f): Funnels of output vectors with and without measurement noises.

5. Conclusions

Dynamic operability corresponds to an output controllability measure that can be used to assist with the formulation of online constrained control problems (Gazzaneo et al., 2020). However, in dynamic operability mapping, exhaustive input discretization methods in the reported literature quickly become intractable with the increase in predictive horizon length. In this work, a novel dynamic operability mapping was proposed in a two-step framework that allows the majority of the computational effort being performed offline. The achievable output sets at different predictive times were formulated as set of inequality constraints that are updated online according to the current full state information and uncertainty propagation. Even though the current framework is limited to a linear time-invariant dynamic process, the proposed theory is a valid basis for future work on linear time-varying and nonlinear dynamic processes.

References

Barber, C.B., Dobkin, D.P., Huhdanpaa, H., 1996. The Quickhull Algorithm for Convex Hulls. ACM Transactions on Mathematical Software (TOMS) 22, 469–483.

Fukuda, K., Prodon, A., 1996. Double Description Method Revisited, in: Deza, M., Euler, R., Manoussakis, I. (Eds.), Combinatorics and Computer Science, Lecture Notes in Computer Science. Springer Berlin Heidelberg, Berlin, Heidelberg, pp. 91–111.

Gazzaneo, V., Carrasco, J.C., Vinson, D.R., Lima, F.V., 2020. Process Operability Algorithms: Past, Present, and Future Developments. Ind. Eng. Chem. Res. 59(6), 2457–2470.

Lima, F.V., Georgakis, C., 2009. Dynamic Operability for the Calculation of Transient Output Constraints for Non-Square Linear Model Predictive Controllers. IFAC Proceedings Volumes 42(11), 231–236.

Muller, D.E., Preparata, F.P., 1978. Finding the Intersection of Two Convex Polyhedra. Theoretical Computer Science 7, 217–236.